

Comparison of Conventional US and Spatial Compound Imaging in Diagnostic Performances of Computer Aided Diagnosis System

Wei-Chih Shen
Dept. of Computer Science and
Information Engineering, Asia
University
Taichung County, Taiwan
wcshe@gmail.com

Ruey-Feng Chang
Dept. of Computer Science and
Information Engineering, National
Taiwan University
Taipei, Taiwan
rfchang@csie.ntu.edu.tw

Woo Kyung Moon
Dept. of Radiology and Clinical
Research Institute, Seoul National
University Hospital
Seoul, Korea
moonwk@radcom.snu.ac.kr

Abstract

To compare the diagnostic performances between two computer aided diagnosis (CAD) systems, this research trains one system by conventional ultrasound (US) and the other by spatial compound imaging, for differentiating between benign and malignant breast masses. The study obtains conventional US and spatial compound images in 128 patients with 140 masses including ninety-seven benign and forty-three malignant masses simultaneously. Each mass was characterized by eight computerized features including the morphological class (shape, orientation, and margin) and acoustic class (lesion boundary, echo pattern, and posterior shadowing). The study trained the binary logistic regression model by correlating the pathological results with the computerized features as a CAD system. When utilizing acoustic class features to construct CAD systems, the area indices under ROC curves were 0.80 and 0.85, respectively, using conventional ultrasound and using spatial compound imaging. The area indices were 0.95 and 0.97, respectively, using all features in conventional US and that in spatial compound imaging. The diagnostic performance of the CAD system did not significantly improved using spatial compound imaging.

1. Introduction

Ultrasound imaging has become more prevalent than other medical imaging techniques due to convenience, noninvasiveness, and forming images in real-time. For breast ultrasound findings, the Breast Imaging Reporting and Data System (BI-RADS) developed by the American College of Radiology [1] standardizes the descriptions of sonographic characteristics and treatments as lexicon. Clinically, the radiologist describes the US finding on the basis of standardized descriptions in BI-RADS including shape, orientation, margin, lesion boundary, echo pattern, and posterior shadowing features and then assess the likelihood of malignancy.

However, the ultrasound image suffers from an inherent imaging artifact called speckle. Generally, the speckle artifact in an image masks the details and degrades contrast. To reduce this artifact, spatial compound imaging was, therefore, proposed [2-4]. Electronic beam steering of a transducer array rapidly acquires and compounds several images of the same region from varying insonation angles to form an image

at real-time frame rates. The formed image is averaged from images at several different angles, reducing speckle artifact influence.

Compared with conventional US, using spatial compound imaging could improve image quality [5-8]. The improvements include reducing speckle artifacts, enhancing mass margin delineation, and improving the conspicuity of low-contrast mass. However, the posterior acoustic characteristic is less clear in spatial compound imaging than in conventional US. Differences between the two imaging techniques have concerned radiologists regarding the inter-observer agreement [9, 10]. In their results, using spatial compound imaging improves the inter-observer agreement and reduces the inter-observer variation. Further, Cha et al. [11] assessed the influence of spatial compound imaging for diagnostic performance of radiologists. They concluded that spatial compound imaging did not significantly improve diagnostic performance of radiologists with respect to characterizing solid breast masses.

With the rapid development of computer applications, computer-aided diagnosis (CAD) systems were widely developed for differentiating the benign from malignant masses [12-15]. In these results, several computerized features were defined to characterize the mass and the correlation with corresponding pathological results was regressed by training a classification model, such as a neural network, as a CAD system [12, 14]. However, research investigating the influences of imaging techniques to a CAD system is lacking. This study assesses the influences of spatial compound imaging, compared with the conventional US, for the CAD system.

2. Materials and Methods

2.1. Data Acquisition

This research obtained approval from the institutional review board and consent from all patients included in this study. Between December 2002 and February 2003, 128 patients underwent excisional or percutaneous needle biopsy due to suspicious mammographic or physical findings examined by ultrasound. An experienced breast radiologist using an ultrasound scanner ATL HDI 5000 (Advanced Technological Laboratory, Bothell, WA, USA) performed the ultrasound examinations. This study included a total of

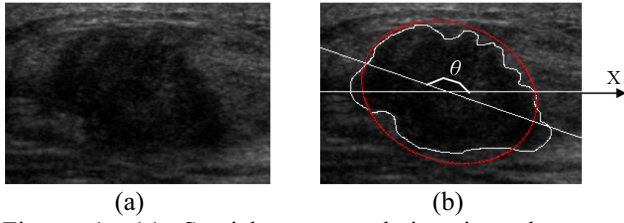


Figure 1. (a) Spatial compound imaging shows a malignant US finding. (b) The best-fit ellipse is regarded as baseline to describe the mass shape and orientation.

140 solid breast masses, including ninety-seven benignities and forth-three malignancies. The scanning processes used linear-array transducers with a 5-12 MHz and did not use changing depth, focus position, and gain settings. Both conventional US and spatial compound imaging captured images and randomly determined the order of acquisitions. The target mode produced all spatial compound images consisting of nine frames obtained from different viewing angles. The scanning protocol used both transverse and longitudinal real-time imaging of the solid masses and a split-screen imaging mode obtained identical images with conventional US and spatial compound imaging. To avoid interaction between computerized image segmentation methods and imaging techniques, the radiologist retrospectively analyzed static ultrasound images and drew the margin of mass using a paint program (Microsoft Paint, version 5.2, Microsoft Inc, Seattle, WA).

2.2. Computerized BI-RADS Features

The BI-RADS sonographic features, including shape, orientation, margin, lesion boundary, echo pattern and posterior shadowing, are quantified into eight computerized features to characterize a mass.

The best-fit ellipse [16] characterizes the mass shape as shown in Fig. 1. The ratio between the perimeter of mass and that of corresponding best-fit ellipse evaluates the irregularity, S_{PR} , for a mass shape as

$$S_{PR} = \frac{Perimeter(mass)}{Perimeter(best-fit\ ellipse)} \quad (1).$$

Further, the mass orientation, O_E , can be estimated by the angle θ between the horizontal line and the major-axis of the best-fit ellipse as shown in Fig. 1. The range of θ is limited in $[0, \pi/2]$.

The distance map [16] counts the undulations and angular characteristics on the mass margin. For each pixel in the ROI, the distance to the lesion boundary is calculated. Fig. 2(b) shows an example for the distance map of a mass. In the figure, darker intensity means a longer distance. The lobulate areas between the mass margin and the maximum inscribed circle of the mass are defined as candidates of undulation as shown in Fig. 2(c). If the maximum distance within each lobulate area is larger than a predefined threshold, this lobulation is admitted to an undulation. The local maxima on the distance map are grouped and each formed group is regarded as an angular characteristic as shown in Fig. 2(c). Finally, this research regards the summation of undulations and angular characteristics, M_{UA} , are regarded as a margin feature.

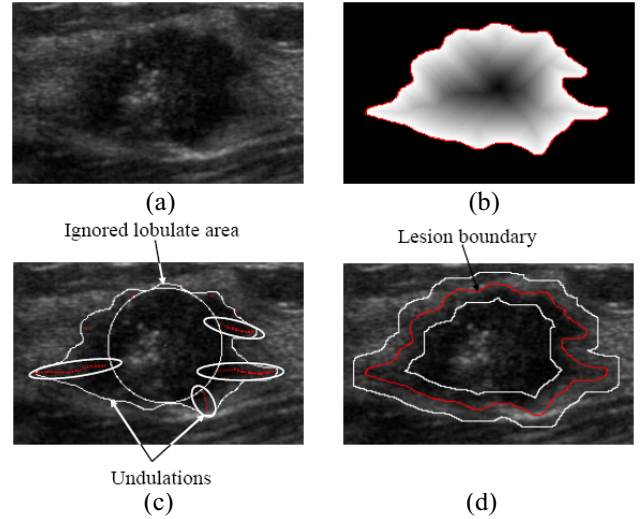


Figure 2. (a) Spatial compound imaging shows a malignant US finding. (b) The corresponding distance map of mass (a). (c) Two undulation and four angular characteristics are discovered on the margin. Each angular characteristic is circumscribed by ellipse. (d) Outer and inner areas around the lesion boundary also could be partitioned by distance map..

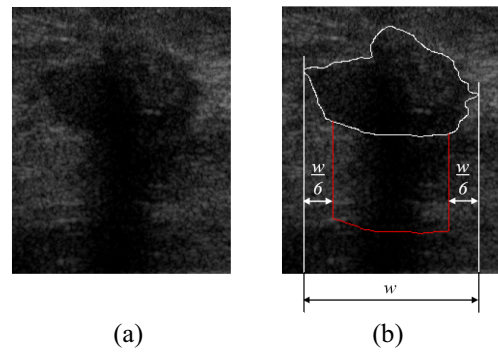


Figure 3. (a) Conventional US shows an US finding. (b) The area behind the mass is defined to evaluate the posterior acoustic characteristic.

For evaluating the degree of abrupt interface across a lesion boundary, the distance map partitions two disjointed ring-like areas around the lesion boundary as shown in Fig. 2(d). The difference between the average gray intensities of two areas evaluates the degree of abrupt interface, LB_D .

The contrast and variation within a mass measure echo pattern characteristic is measured by the. When sorting the pixels within the mass in ascendant order by their gray intensities, the first quartile Q_1 is computed in order to divide the pixels into darker and general groups. The average gray intensities for the mass and darker group are defined as

$$avg_mass = \frac{\sum I(p)}{N_{MP}} \quad \text{and} \quad avg_DG = \frac{\sum_{I(p) \leq Q_1} I(p)}{N_{DG}} \quad (2)$$

where N_{MP} is the number of mass pixels and N_{DG} is the number of pixels in the darker group and $I(p)$ indicates the gray intensity of pixel I . Then, the contrast feature EP_C is defined as

$$EP_C = \frac{avg_DG}{avg_mass} \quad (3).$$

Table 1. The mean value and standard deviation of each computerized BI-RADS feature in the benign and the malignant groups. The difference between two groups was evaluated by Student's t-test.

Feature	Conventional US			Spatial compound imaging		
	Benign	Malignant	<i>p</i> -value	Benign	Malignant	<i>p</i> -value
S_{PR}	0.99±0.08	1.23±0.17	<0.001	0.99±0.06	1.18±0.15	<0.001
O_E	8.20±7.70	16.10±17.45	0.006	8.26±8.18	14.47±16.16	0.021
M_{UA}	3.82±1.24	9.95±3.30	<0.001	4.04±1.28	8.58±2.84	<0.001
LB_D	23.60±6.56	17.05±4.79	<0.001	23.36±7.19	14.31±6.09	<0.001
EP_C	0.44±0.21	0.34±0.24	0.011	0.51±0.19	0.42±0.23	0.018
EP_{AG}	50.16±10.42	44.97±10.97	0.008	39.73±7.36	35.35±7.80	0.002
PS_C	33.04±7.53	29.94±6.98	0.023	33.73±10.04	28.29±9.13	0.003
PS_{AG}	72.03±17.20	58.81±16.64	<0.001	60.48±19.11	43.33±14.16	<0.001

The variation on pixel $p(x, y)$ can be evaluated by the gradient magnitude. Further, the variation of a mass, EP_{AG} , can be measured as

$$EP_{AG} = \frac{\sum G(p)}{N_{MP}} \quad (4)$$

where $G(p)$ is the gradient magnitude at pixel p .

The posterior area behind the mass is defined for evaluating the posterior acoustic characteristic as shown in Fig. 3. For avoiding edge shadowing, the left and right boundaries of the posterior area are, respectively, shrunk one-sixth of the mass width. The top and bottom boundaries of the posterior area are parallel to the bottom boundary of mass. When sorting the pixels within the posterior area in ascendant order by their gray intensities, the third quartile Q_3 is computed in order to divide them into brighter and general groups. The average gray intensities for the posterior area and brighter group are defined as

$$avg_PA = \frac{\sum I(p)}{N_{PA}} \quad \text{and} \quad avg_BG = \frac{\sum_{I(p) \geq Q_3} I(p)}{N_{BG}} \quad (5)$$

where N_{PA} is the number of pixels in the posterior area and N_{BG} is the number of pixels in the brighter group. The contrast feature PS_C is then defined as

$$PS_C = avg_BG - avg_PA \quad (6)$$

The variation of posterior area PS_{AG} is also evaluated by the average of gradient magnitudes as

$$PS_{AG} = \frac{\sum G(p)}{N_{PA}} \quad (7)$$

2.3. Experiments and performance evaluations

The identification ability of conventional US and that of spatial compound imaging in differentiating between malignant and benign masses were validated by Student's t-test. Before calculating the Student's t-test, this work performed the Levene's test to verify the equality of variances.

The defined computerized BI-RADS features represented both conventional US and spatial compound imaging. For each imaging technique, the current work trained the binary logistic regression model [17] by correlating the pathological results with the computerized BI-RADS features as a CAD system. In the defined computerized BI-RADS features, the acoustic related features, including lesion boundary, echo pattern, and posterior acoustic characteristic, reflect the difference

between two imaging techniques of the suspicious mass. The other features mainly present the radiologists' perception. Therefore, this study also uses the acoustic related features to construct a CAD system respectively in either imaging technique.

The k-fold cross validation method [18] verifies the diagnostic performance of the constructed CAD system. In this study, $k=10$, the adopted cases are randomly partitioned into ten sets according to the pathological result. The numbers of benign and malignant cases in each set is similar. The current work regards each set as the test set once and diagnosed by the CAD system trained by the remaining nine sets. Five performance indices, including accuracy, sensitivity, specificity, positive predictive value (PPV), and negative predictive value (NPV), evaluated diagnostic performance of the constructed CAD system. For each performance index, the Chi-square test measured the significance of difference between two resulting values. The ROC analysis also measured diagnostic performance of the CAD system [19]. The z-test measured the significance of difference between two resulting Az values.

3. Results

Table 1 lists the mean value and standard deviation in the benign and malignant groups for conventional US and spatial compound imaging on each computerized BI-RADS feature. According to the resulting p -values in the Student's t test, the benign masses group was statistically different from the malignant group on each BI-RADS feature either for conventional US or spatial compound imaging because all p -values are less than 0.001 or 0.05.

When using acoustic related features to construct a CAD system, the current study merged the predicted likelihoods of malignancy in the ten test sets as the final diagnostic results for each imaging technique. The area index under the ROC curve was 0.80 for the CAD systems using conventional US compared to the area 0.85 for those at spatial compound imaging as shown in Fig. 4. The difference between the two area indices was 0.05 and not significant because the p -value was 0.148 in the z-test. The diagnostic performances, accuracy, sensitivity, specificity, PPV, and NPV of final diagnostic results for conventional US were 73.6(103/140), 74.4(32/43), 73.2(71/97), 55.2(32/58), and 86.6(71/82) respectively. Oppositely, the corresponding performances were 79.3(111/140), 83.7(36/43), 77.3(75/97), 62.1(36/58), and 91.5(75/82) respectively. Although all indices for spatial compound imaging were better than another technique, the differences were not statistically significant because all p -values were larger than 0.05 in the Chi-square test.

When adopting all computerized BI-RADS features, this work further compared the CAD systems trained by conventional US and those trained by spatial compound imaging. The area index under the ROC curve was 0.97 for conventional US compared to the area index 0.95 for spatial compound imaging as shown in Fig. 4. The difference between the two area indices was not significant because the p -value was 0.546 in the z-test. The diagnostic performances, accuracy, sensitivity, specificity, PPV, and NPV of final diagnostic results for

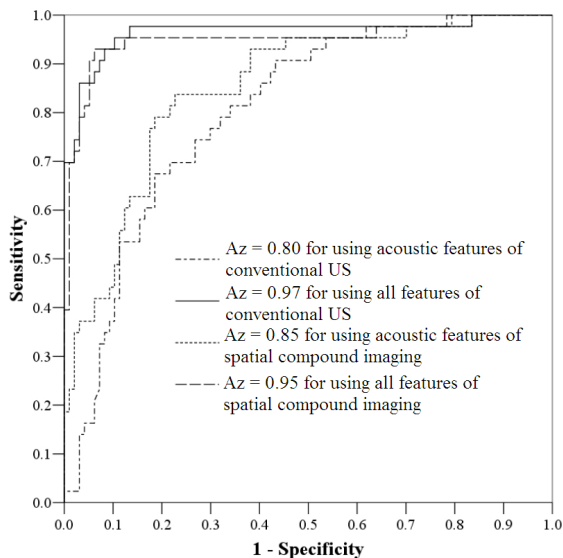


Figure 4. The ROC curves for four CAD systems constructed by using conventional US or by using spatial compound imaging. For each imaging technique, two CAD systems are respectively trained by using acoustic features and by using all features.

conventional US were 92.1(129/140), 93.0(40/43), 91.8(89/97), 83.3(40/48), and 96.7(89/92) respectively. For spatial compound imaging, the corresponding indices were 93.6(131/140), 93.0(40/43), 93.8(91/97), 87.0(40/46), and 96.8(91/94). The differences were also not statistically significant in the Chi-square test.

4. Discussion

In this study, the US findings either for conventional US or for spatial compound imaging were characterized by eight computerized BI-RADS features. In terms of capability for differentiating the malignant from benign masses, both conventional US and spatial compound imaging were statistically significant in the Student's t-test, respectively. For the CAD system either trained by conventional US or trained by spatial compound imaging, the capabilities for diagnosing masses were not statistically significant regardless of using acoustic related features or using all features.

Acknowledgments

This work was supported by National Science Council, Taiwan (Grant NSC 97-2221-E-468-007).

References

[1] American College of Radiology (ACR). Breast Imaging Reporting and Data System Third Edition. Reston (VA): American College of Radiology, 2003.
 [2] Burckhardt CB. Speckle in ultrasound B-mode scans. IEEE. Trans. Sonics Ultrason. 1978; SU-25:1.

[3] Trahey GE, Smith SW, Von Ramm OT. Speckle pattern correlation with lateral aperture translations: experimental results and implications for spatial compounding. IEEE Trans. Ultr. Ferr. Freq. 1986; 33:257-264.
 [4] Jespersen SK, Wilhjelm JE, Sillesen H. Multi-angle compound imaging. Ultrason Imaging. 1998; 20:81-102.
 [5] Behar V, Adam D, Friedman Z. A new method of spatial compounding imaging. Ultrasonics 2003; 41:377-384.
 [6] Oktar SO, Yucel C, Ozdemir H, et al. Comparison of conventional sonography, real-time compound sonography, tissue harmonic sonography, and tissue harmonic compound sonography of abdominal and pelvic lesions. AJR Am J Roentgenol 2003; 181:1341-1347.
 [7] Lacefield JC, Pilkington WC, Waag RC. Comparisons of lesion detectability in ultrasound images acquired using time-shift compensation and spatial compounding. IEEE Trans Ultrason Ferroelectr Freq Control 2004; 51:1649-1659.
 [8] Rickes S, Bohm J, Malfertheiner P. SonoCT improves on conventional ultrasound in the visualization of the pancreatic and bile duct: A pilot study. J Gastroenterol Hepatol. 2006; 21:552-555.
 [9] Kofoed SC, Gronholdt ML, Wilhjelm JE, et al. Real-time spatial compound imaging improves reproducibility in the evaluation of atherosclerotic carotid plaques. Ultrasound Med Biol. 2001; 27:1311-1317.
 [10] Seo BK, Oh YW, Kim HR, et al. Sonographic evaluation of breast nodules: comparison of conventional, real-time compound, and pulse-inversion harmonic images. Korean J Radiol. 2002 ; 3:38-44.
 [11] Cha JH, Moon WK, Cho N, et al. Differentiation of benign from malignant solid breast masses: conventional US versus spatial compound imaging. Radiology 2005; 237:841-846.
 [12] Chen DR, Chang RF, Huang YL. Computer-aided diagnosis applied to US of solid breast nodules by using neural networks. Radiology 1999; 213:407-412.
 [13] Horsch K, Giger ML, Venta LA, et al. Computerized diagnosis of breast lesions on ultrasound. Med Phys 2002; 29: 157-164.
 [14] Chen CM, Chou YH, Han KC, et al. Breast lesions on sonograms: computer-aided diagnosis with nearly setting-independent features and artificial neural networks. Radiology 2003; 226:504-514.
 [15] Shen WC, Chang RF, Moon WK, Chou YH, Huang CS. Breast ultrasound computer-aided diagnosis using BI-RADS features. Acad Radiol. 2007 Aug; 14(8):928-39.
 [16] Jain AK. Fundamentals of Digital Image Processing. Prentice-Hall, 1989.
 [17] Hosmer DW, Lemeshow S. Applied Logistic Regression 2nd Edition. Wiley, 2000.
 [18] Stone M. Cross-validatory Choice and Assessment of Statistical Predictors. Journal of the Royal Statistical Society. 1974; 36:111-147.
 [19] Hanley JA, McNeil BJ. A method of comparing the areas under receiver operating characteristic curves derived from the same cases. Radiology. 1983; 148:839-843.